Environmental Research Communications

PAPER

Leaf-level chlorophyll fluorescence and reflectance spectra of high latitude plants

K Fred Huemmrich[1,*] , Petya Campbell[2], Sergio A Vargas Z[3] , Sarah Sackett[4], Steven Unger[5] , Jeremy May[6], Craig Tweedie[7] and Elizabeth Middleton[8]

[1] University of Maryland Baltimore County, Joint Center for Earth Systems Technology, Baltimore, MD 21228 United States of America
[2] University of Maryland Baltimore County, Joint Center for Earth Systems Technology, Baltimore, MD 21228 United States of America
[3] University of Texas at El Paso, Environmental Science and Engineering Program, El Paso, TX 79968, United States of America
[4] NASA Carbon Cycle & Ecosystems Office, 2367 University Ave S Fairbanks, AK 99709, United States of America
[5] Florida International University, Department of Biological Sciences, Miami, FL 33199, United States of America
[6] Florida International University, Department of Biological Sciences, Miami, FL 33199, United States of America
[7] University of Texas at El Paso, Environmental Science and Engineering Program, El Paso, TX 79968, United States of America
[8] NASA Goddard Space Flight Center, Code 618, Greenbelt, MD 20771, United States of America
* Author to whom any correspondence should be addressed.

E-mail: huemmric@umbc.edu

Keywords: fluroescence, hyperspectral, tundra, boreal forest

Abstract

Little is known about the chlorophyll fluorescence spectra for high latitude plants. A FluoWat leaf clip was used to measure leaf-level reflectance and chlorophyll fluorescence spectra of leaves of common high latitude plants to examine general spectral characteristics of these species. Fluorescence yield (Fyield) was calculated as the ratio of the emitted fluorescence divided by the absorbed radiation for the wavelengths from 400 nm up to the wavelength of the cut-off for the FluoWat low pass filter (either 650 or 700 nm). The Fyield spectra grouped into distinctly different patterns among different plant functional types. Black spruce (*Picea mariana*) Fyield spectra had little red fluorescence, which was reabsorbed in the shoot, but displayed a distinct far-red peak. Quaking aspen (*Populus tremuloides*) had both high red and far-red Fyield peaks, as did sweet coltsfoot (*Petasites frigidus*). Cotton grass (*Eriophorum* spp.) had both red and far-red Fyield peaks, but these peaks were much lower than for aspen or coltsfoot. Sphagnum moss (*Sphagnum* spp.) had a distinct Fyield red peak but low far-red fluorescence. Reindeer moss lichen (*Cladonia rangiferina*) had very low fluorescence levels, although when damp displayed a small red Fyield peak. These high latitude vegetation samples showed wide variations in Fyield spectral shapes. The Fyield values for the individual red or far-red peaks were poorly correlated to chlorophyll content, however the ratio of far-red to red Fyield showed a strong correlation with chlorophyll content. The spectral variability of these plants may provide information for remote sensing of vegetation type but may also confound attempts to measure high latitude vegetation biophysical characteristics and function using solar induced fluorescence (SIF).

1. Introduction

High latitudes are experiencing significant climate change effects and as a result tundra and boreal forest ecosystems are expected to respond to climate induced environmental variability, both in terms of shifts in plant species composition and in their physiological responses (e.g., Prevéy *et al* 2017, Myers-Smith *et al* 2011, 2020). Due to its vast extent and difficulties of accessibility, low Earth orbit (LEO) remote sensing from satellites, as well as from aircraft, are important tools for describing high latitude ecosystem characteristics and change over time (Beamish *et al* 2020).

High latitude vegetation is dominated by tundra and taiga woodlands, which are frequently composed of combinations of nonvascular and vascular vegetation. Spatial and spectral information on these ecosystems is sparse. Nonvascular vegetation, such as lichens and mosses, physiologically respond differently than vascular

plants (Green & Lange 1995, Tenhunen *et al* 1995) and have different spectral reflectance characteristics than vascular plants (Stow *et al* 1993, Hope & Stow 1996). Further, evergreen conifers, such as black spruce, are common in boreal forests and due to their needle, shoot, and canopy characteristics add complexities to interpretation of spectral reflectance properties, which also differ from broadleaf temperate species (Williams 1991, Rautiainen *et al* 2018). In addition to mapping these plant types there is the challenge to utilize the remotely acquired observations to estimate physiological function, such as carbon capture.

Advanced remote sensing approaches have the potential to dramatically improve descriptions of high latitude ecosystems. Imaging spectrometers provide information on both the shape and magnitude of spectral reflectance, and solar induced fluorescence (SIF) can be determined using very narrow band spectrometers. Data from these types of measurements can be used to retrieve vegetation cover types and productivity (Middleton 2018, Mohammed *et al* 2019). The reflectance spectra of high latitude plant functional types (e.g. lichens, mosses, and vascular plants) differ enough to allow spectral unmixing to determine cover fractions (Huemmrich *et al* 2013, Bratsch *et al* 2016, 2017). Satellite derived SIF have been used in top-down approaches to develop global relationships with gross primary production (GPP) (Frankenberg *et al* 2011, Guanter *et al* 2012, Joiner *et al* 2014) as well as specifically for boreal forest regions (Jeong *et al* 2017). However, the reflectance spectra of high latitude vegetation are highly variable, and the characteristics of their chlorophyll fluorescence spectra are poorly known and thus represent potential sources of uncertainty (Buchhorn *et al* 2013, Bratsch *et al* 2016, 2017).

The shape of typical healthy green leaf chlorophyll fluorescence spectra has two broad maxima with one in the red spectral region around 685–690 nm and the other in the far-red (near-infrared) spectral region around 730–740 nm. This spectral shape is related to two photosystems: PSII, which emits in both the red and far- red regions, and PSI, which emits mainly in the far-red, providing a relationship between fluorescence spectral characteristics, chlorophyll content, and photosynthesis (Murata *et al* 1966, Boardman *et al* 1991, Pfündel 1998). The red peak is often lower than the far-red peak, due to re-absorption of fluoresced red light by chlorophyll within the leaf. The emitted SIF flux is a small signal relative to reflected solar radiation, representing about 2%– 5% of the reflected radiance in the near infrared (Mohammed *et al* 2019). The overall intensity of emitted SIF depends mainly on incoming radiation and chlorophyll concentration (Middleton 2018, Mohammed *et al* 2019).

Interpretation of remotely acquired observations of landscapes requires linking with known properties of the vegetation in that landscape. The full use of these state-of-the-art optical remote sensing techniques begins with a description and improved understanding of leaf level optical reflectance and chlorophyll fluorescence characteristics of dominant vegetation cover types. To advance this effort we used an ASD spectrometer attached to a FluoWat leaf clip to make consistent measurements of reflectance and chlorophyll fluorescence spectra of common high latitude plants to examine general spectral characteristics of these species.

2. Methods

2.1. Fluowat measurements

The FluoWat leaf clip is designed to make consistent reflectance and fluorescence spectral measurements (Van Wittenberghe *et al* 2013, 2015). In use, the open port of the clip was aimed directly at an illumination source which illuminated the plant sample held in the clip at a consistent 45° angle to the fiber optic connected to the spectrometer (Analytical Spectral Devices (ASD) FieldSpec 3, Malvern Panalytical, Analytik Ltd; Cambridge, United Kingdom). In this study a halogen light source was used to illuminate the samples. Spectral reflectance measurements were collected from measurements with an open illumination port. Fluorescence spectra measurements were collected with the illumination port covered with one of two low pass filters. In these measurements the two filters had either a 650 nm or a 700 nm cut off wavelength. These filters blocked all incident light above the cut off wavelength, so that the only photons reaching the sensor in these longer wavelengths (greater than 650 or 700 nm) were due to fluorescence emitted from the sample.

In the FluoWat measurements we attempted to completely fill the spectrometer field of view with the plant sample. This was straightforward for plants with large leaves, and when possible, single leaves were measured. For smaller or narrow leaves, such as grasslike leaves, two or more leaves were arranged side by side to fill the field of view, while avoiding overlaps or gaps between leaves as much as possible. For the conifer samples, entire shoots including twigs and needles were placed in the FluoWat clip for measurement. Samples of mosses and lichens were placed in the clip filling the field of view and arranged so the light was illuminating the tops of the mats.

Using the FluoWat clip, measurements of radiance from both the leaf top and leaf bottom (reflectance and transmittance) can be collected. However, due to the nature of the plant samples in this study, with small leaves
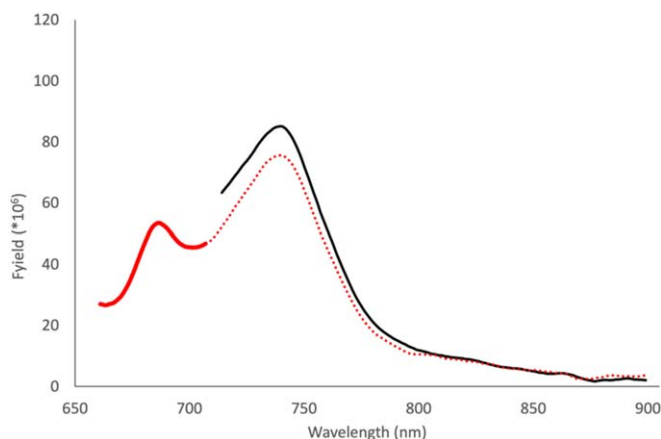
Figure 1. Sample leaf Fyield (x10^6) from the FluoWat leaf clip. The red lines, both solid and dashed, describe the Fyield derived using only the 650 nm filter. The solid black line is the Fyield derived using the 700 nm filter. The combination of the solid red and black lines represents the data presented in the Fyield figures below (figures 3(B) and 5(A)–(F)) with a 6 nm gap between the Fyields from the different filters.

on the conifers, herbaceous tundra plants, and no leaves on the mosses and lichens, we report only the reflectance and fluorescence from the upper (top or adaxial) surfaces.

Reflectance (Refl$_\lambda$) for each wavelength, λ, was calculated as:

$$Refl_\lambda = \frac{(R_\lambda - D_\lambda)}{(C_\lambda - D_\lambda)} \tag{1}$$

Where R_λ is the reflected radiance, D_λ is the dark measurement, and C_λ is the calibration panel radiance.

Fluorescence yield (Fyield$_\lambda$) was calculated as:

$$Fyield_\lambda = \frac{(F_\lambda - D_\lambda)}{APAR} \tag{2}$$

Where F_λ is the emitted radiance measured with a filter across the illumination port, D_λ is the dark measurement, and APAR is the sum of the absorption for the wavelengths from 400 nm to the filter cut off wavelength (either 650 or 700 nm). In the figures below the plotted Fyield values are multiplied by 10^6. In the calculation of the Fyield spectra, wavelengths from 659 to 709 nm were measured using the 600 nm low pass filter to cover the wavelengths of the fluorescence red peak, and the Fyield for wavelengths longer than 712 nm were measured using the 700 nm filter for the fluorescence far-red peak. The use of the 700 nm filter allows incident light transmittance through the filter to the sample in the important red spectral bands for chlorophyll absorption. Figure 1 provides an example of the difference in the far-red Fyield between the 650 versus 700 nm filters. A 6 nm gap has been placed in the Fyield spectra plots from 708 to 713 nm to indicate the transition from Fyields measured with the 650 nm filter versus those using the 700 nm filter (figure 1). These Fyield spectra were smoothed using a five-point running average.

2.2. Chlorophyll measurements

Chlorophyll content was measured using a CCM-300 Chlorophyll Content Meter (Opti-Sciences, Hudson, NH, USA). Unlike other types of chlorophyll sensors, the CCM-300 does not use transmitted light, rather the CCM emits a beam of light at ∼460 nm for excitation and measures the fluorescence emissions at ∼700 and 735 nm through a fiber optic probe. Chlorophyll concentration is determined by a linear relationship to the ratio of F735/F700 (Gitelson *et al* 1999). Thus, the CCM-300 is appropriate to measure materials such as lichens and mosses where measurements of transmittance are problematic. The reported chlorophyll content values are the averages of five measurements with the CCM-300.

2.3. Plant sampling

Plant samples were harvested from areas around Fairbanks (near 64.86°N, −147.86°E), Utqiaġvik (near 71.32°N, −156.67°E), and Toolik Lake (near 68.62°N, −149.60°E), AK, USA during the summers of 2019, 2020, and 2021.

In the boreal forest near Fairbanks conifers are predominately white (Picea glauca) and black spruce (P. mariana), with larch (Larix laricina) found in some localities. Important deciduous trees are trebling aspen (Populus tremuloides), balsam poplar (P. balsamifera), and birch (Betula neoalaskana). Shrubs include alders

Table 1. Summary of samples measured with the FluoWat.

Common name	Scientific name	Functional type	Number of samples
Reindeer moss	*Cladonia rangiferina*	Lichen	7
Sphagnum moss	*Sphagnum spp.*	Moss	14
Feather moss	*Hylocomnium splendens*	Moss	3
Black spruce	*Picea mariana*	Conifer	11
Tamarack	*Larix laricina*	Conifer	1
White spruce	*Picea glauca*	Conifer	4
Cotton grass	*Eriophorum spp.*	Herbaceous plant	6
Water sedge	*Carex aquatilis*	Herbaceous plant	5
Sweet coltsfoot	*Petasites frigidus*	Herbaceous plant	9
Pendant grass	*Arctophila fulva*	Herbaceous plant	2
Vaccinium heath	*Vaccinium vitis-idaea*	Evergreen shrub	6
Alpine bearberry	*Arctous alpina*	Evergreen shrub	3
Arctic bell-heather	*Cassiope tetragona*	Evergreen shrub	2
Labrador tea	*Rhododendron tomentosum*	Evergreen shrub	1
Tealeaf willow	*Salix pulchra*	Deciduous shrub/tree	6
Dwarf birch	*Betula nana*	Deciduous shrub/tree	2
Birch spp.	*Betula spp.*	Deciduous shrub/tree	2
Quaking aspen	*Populus tremuloides*	Deciduous shrub/tree	8
Green alder	*Alnus viridis*	Deciduous shrub/tree	5

(Alnus spp.) and willows (Salix spp.). Nonvascular mosses and lichens are important components of the understory (Smith 2008).

The land cover at Utqiaġvik is primarily coastal acidic tundra, dominated by sedge herbaceous cover in wetlands. Common vascular species include water sedge (Carex aquatilis), cottongrass (Eriophorum vaginatum) and tundra grass (Dupontia fisheri), along with some shrubs (Salix spp.). Mosses are a significant portion of the community and represent a significant fraction of the ground cover (Brown *et al* 1980, Hollister *et al* 2005).

The Toolik region is predominately tussock tundra with abundant sedges (Carex bigelowii) and tussock cottongrass (Eriophorum vaginatum). Low shrubs, including dwarf birch (Betula glandulosa or nana) and tealeaf willow (Salix pulchra) are also common along with heaths (Vaccinium vitis-idaea) (Walker *et al* 1994).

Mosses and lichens were sampled by removing small areas of the mats (~5 cm square) including the underlying soil. Herbaceous plants were sampled by digging up their roots and soil ball. Twigs were cut from shrubs and trees. The cut ends were wrapped with wet paper towels. Immediately following harvesting, the samples were stored in plastic bags or containers, kept hydrated, and express mailed to Maryland, where they were measured within days of arrival. The aim was to collect a set of samples representing major types of plant cover for these high latitude regions and are summarized in table 1.

These measurements were compared with sample FluoWat leaf measurements of temperate species including corn (*Zea mays*) and temperate forest trees. Corn leaves were measured *in situ* using direct solar illumination at the United States Department of Agriculture (USDA) Beltsville Agricultural Research Center (BARC) in Greenbelt, MD, USA. The temperate deciduous tree leaves were measured using the halogen light source at the Smithsonian Environmental Research Center (SERC) in Edgewater, MD, USA.

2.4. Statistical analysis

The statistical significance of the differences in Fyield and chlorophyll content among samples were determined based on an ANOVA general linear model (GLM) analysis (SYSTAT 12.3, SYSTAT Software Inc., San Jose, CA, USA) (Zar 2010). This approach was chosen due to the unbalanced design and uneven number of measured sample types, which occurred due to outliers and missing values in this study. We examined the separation based on values for Fyield of sample plant functional types (i.e., conifer, deciduous, herbaceous, lichen, moss), species, sample sources, and their interactions using this approach.

3. Results

3.1. Spectral reflectance

The visible-near infrared spectral reflectance curves from the illuminated top of the samples are shown in figures 2 and 3. For comparison with results obtained for the Alaskan samples, measurements are first provided of temperate mid-latitude North American species (figures 2(A) and (B)). These reflectance and Fyield curves are typical of green vegetation with the reflectance curves displaying low reflectance with a green peak in the visible

Figure 2. Spectral reflectance (Plot A) and Fyield (x10^6) (Plot B) curves for the upper (adaxial) leaf surfaces obtained with the FluoWat leaf clip for a collection of leaves of common temperate plants of the eastern US. Measured species include tree species: beech (*Fagus grandifolia*), hickory (*Carya spp.*), tulip poplar (*Liriodendron tulipifera*), red maple (*Acer rubrum*), red oak (*Quercus rubra*), sweet gum (*Liquidambar styraciflua*), and a major agricultural crop, corn (*Zea mays*).

wavelengths and a dramatic increase in reflectance at the transition from visible to near infrared wavelengths, while the Fyield spectra has two peaks, one in the red and one in the far-red wavelengths. In comparison high latitude sample measurements exhibit wide variability in spectral reflectance (figures 3(A)–(F)) and Fyield (figures 4(A)–(F)) patterns.

The lichens displayed widely variable spectral reflectance (figure 3(A)) and generally had much higher visible reflectance than is typical of green vascular plants (e.g. figure 2(A)). Most of the lichen samples were hydrated when measured and there was a large change in reflectance between the moist lichen and dry lichen curves (dotted line figure 3(A)). Visually, during the course of the measurements, the lichen samples went from a yellow-green color to more of a yellow-white coloring with drying as seen in the differences in the visible reflectance curves. This change points to the capacity for significant variability in reflectance for lichen dominated landscapes depending on wetness.

The moss samples also represented a range of spectral shapes (figure 3(B)). All samples were moist to the touch when measured. The green mosses generally had reflectance spectral shapes similar to typical green vascular plant leaves, while the colored mosses, with colors ranging from yellow through orange to red, had spectral shapes that lacked strong red-edge changes and so looked similar to the spectral reflectance of bare soils. The feather moss spectra were generally brighter than the green sphagnum across the entire observed wavelength range and, in particular, the feather moss showed higher reflectance in the red chlorophyll absorption region (600–690 nm) than the green sphagnum.

The conifer samples were measured using an entire shoot in the leaf clip, including both needles and branchlets, which produced the typical spectral shapes of green leaves (figure 3(C)). However, due to the way the measurements were collected there may have been overlap and/or gaps between the needles that introduced some variability into the spectra (Middleton *et al* 1997, 1998). Generally, the conifer shoots had lower near infrared and green reflectance than deciduous leaves (figure 3(F)).

The other vascular plants shown in figures 3(D)–(F) have typical green leaf spectral shapes similar to temperate leaves (figure 2(A)). The sweet coltsfoot leaf reflectance spectra displayed a relatively high visible reflectance (figure 3(D)), and visually these leaves were somewhat yellow. One sample of cotton grass also had high visible spectral reflectance (dotted line, figure 3(D)) because that sample was a mixture of live and dead leaves. In figure 3(F), the willow leaves were beginning to senesce at the time of the measurement.

3.2. Fyield spectra
Chlorophyll fluorescence spectra are also measured using the FluoWat leaf clip. The chlorophyll fluorescence spectrum is generally characterized by two broad peaks, one in the red spectral region with a maximum value around 685 nm and a second in the far-red spectral region with a maximum value around 740 nm (figure 2(B)). Presented in figure 4 are the spectra of Fyield for the different Alaskan plants, highlighting their different Fyield spectral shapes. Notice how they compare with the temperate species previously shown in figure 2(B).

Many of these high latitude samples had Fyield spectra significantly different than the two-peak shape of the temperate leaves (figure 2(B)). The lichen samples had a small red peak and fairly flat far-red Fyield spectral shape (figure 4(A)). The green sphagnum sample Fyields had a fairly strong red peak and decreasing values across the far-red spectral region (figure 4(B)). The red and orange sphagnum samples had very low Fyield values, smaller than the lichens, while the feather moss had higher Fyield values than the green sphagnum samples
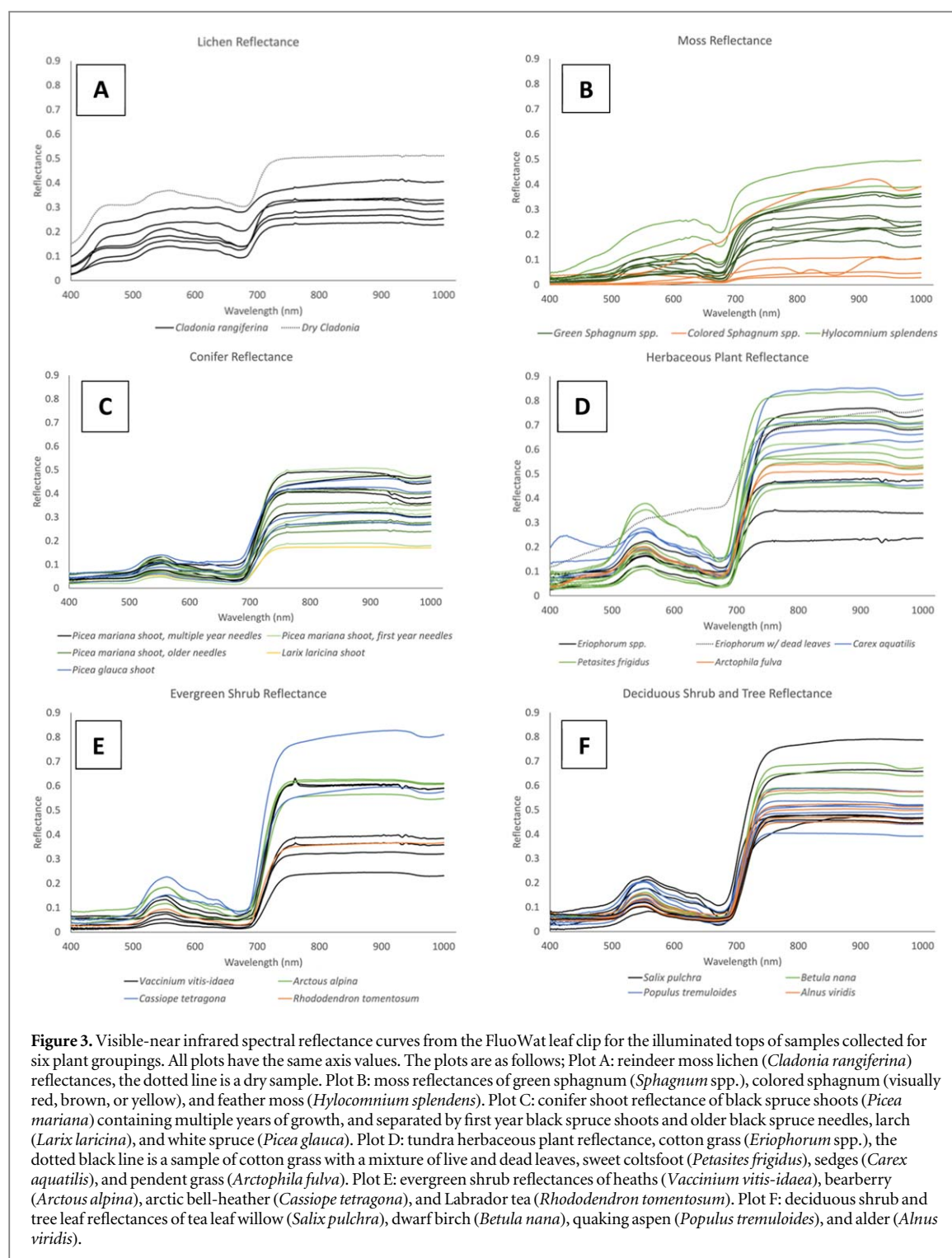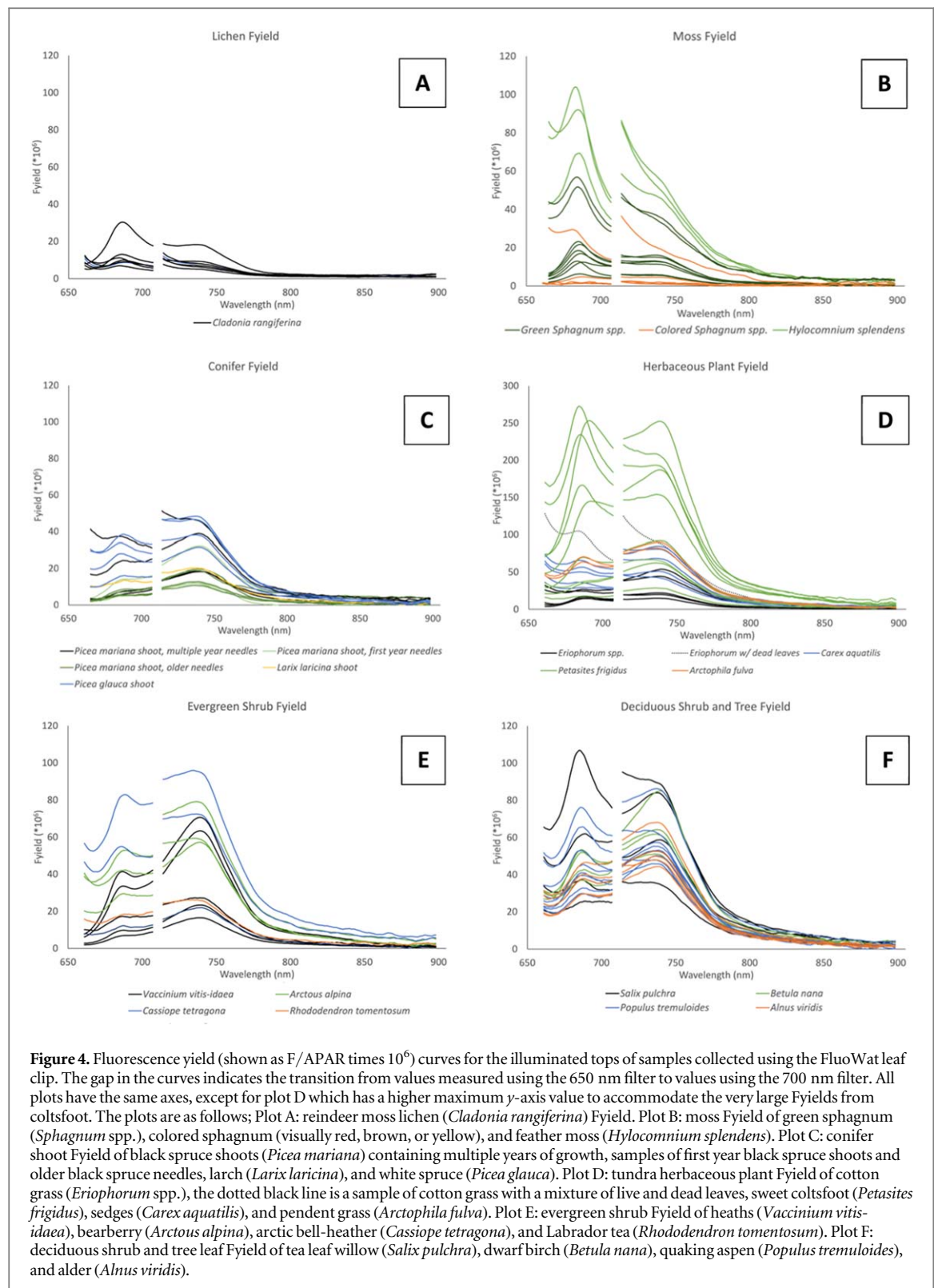
Figure 3. Visible-near infrared spectral reflectance curves from the FluoWat leaf clip for the illuminated tops of samples collected for six plant groupings. All plots have the same axis values. The plots are as follows; Plot A: reindeer moss lichen (*Cladonia rangiferina*) reflectances, the dotted line is a dry sample. Plot B: moss reflectances of green sphagnum (*Sphagnum* spp.), colored sphagnum (visually red, brown, or yellow), and feather moss (*Hylocomnium splendens*). Plot C: conifer shoot reflectance of black spruce shoots (*Picea mariana*) containing multiple years of growth, and separated by first year black spruce shoots and older black spruce needles, larch (*Larix laricina*), and white spruce (*Picea glauca*). Plot D: tundra herbaceous plant reflectance, cotton grass (*Eriophorum* spp.), the dotted black line is a sample of cotton grass with a mixture of live and dead leaves, sweet coltsfoot (*Petasites frigidus*), sedges (*Carex aquatilis*), and pendent grass (*Arctophila fulva*). Plot E: evergreen shrub reflectances of heaths (*Vaccinium vitis-idaea*), bearberry (*Arctous alpina*), arctic bell-heather (*Cassiope tetragona*), and Labrador tea (*Rhododendron tomentosum*). Plot F: deciduous shrub and tree leaf reflectances of tea leaf willow (*Salix pulchra*), dwarf birch (*Betula nana*), quaking aspen (*Populus tremuloides*), and alder (*Alnus viridis*).

across the entire spectral range. In contrast to the green sphagnum, the spruce twig Fyields had no red peaks, but did have clearly defined far-red peaks (figure 4(C)). The cotton grass had clear red and far-red peaks, with the far-red peak larger than the red. The cotton grass sample with the very high visible reflectance due to dead material in the sample (dotted line, figure 2(D)) had the highest Fyield values of all of the cotton grass samples (dotted line, figure 4(D)). The coltsfoot leaves displayed very high red and far-red peaks, so large that the scale for figure 4(D) had to be increased compared to the other sample graphs. The heaths had a Fyield spectral shape similar to the green sphagnum with no red peak and a clear far-red peak (figure 4(E)). The rest of the conifer and deciduous leaves generally displayed two peaked Fyield spectral shapes (figures 4(E) and (F)). The high Fyield values for the willow sample in figure 4(F) may have been due to its senescing condition.

Comparing Fyield red and far-red peak values provides a way to summarize key characteristics of the spectra shown in figure 4 (figure 5). The Alaskan samples have much wider range of values than the temperate samples

Figure 4. Fluorescence yield (shown as F/APAR times 10^6) curves for the illuminated tops of samples collected using the FluoWat leaf clip. The gap in the curves indicates the transition from values measured using the 650 nm filter to values using the 700 nm filter. All plots have the same axes, except for plot D which has a higher maximum *y*-axis value to accommodate the very large Fyields from coltsfoot. The plots are as follows; Plot A: reindeer moss lichen (*Cladonia rangiferina*) Fyield. Plot B: moss Fyield of green sphagnum (*Sphagnum* spp.), colored sphagnum (visually red, brown, or yellow), and feather moss (*Hylocomnium splendens*). Plot C: conifer shoot Fyield of black spruce shoots (*Picea mariana*) containing multiple years of growth, samples of first year black spruce shoots and older black spruce needles, larch (*Larix laricina*), and white spruce (*Picea glauca*). Plot D: tundra herbaceous plant Fyield of cotton grass (*Eriophorum* spp.), the dotted black line is a sample of cotton grass with a mixture of live and dead leaves, sweet coltsfoot (*Petasites frigidus*), sedges (*Carex aquatilis*), and pendent grass (*Arctophila fulva*). Plot E: evergreen shrub Fyield of heaths (*Vaccinium vitis-idaea*), bearberry (*Arctous alpina*), arctic bell-heather (*Cassiope tetragona*), and Labrador tea (*Rhododendron tomentosum*). Plot F: deciduous shrub and tree leaf Fyield of tea leaf willow (*Salix pulchra*), dwarf birch (*Betula nana*), quaking aspen (*Populus tremuloides*), and alder (*Alnus viridis*).

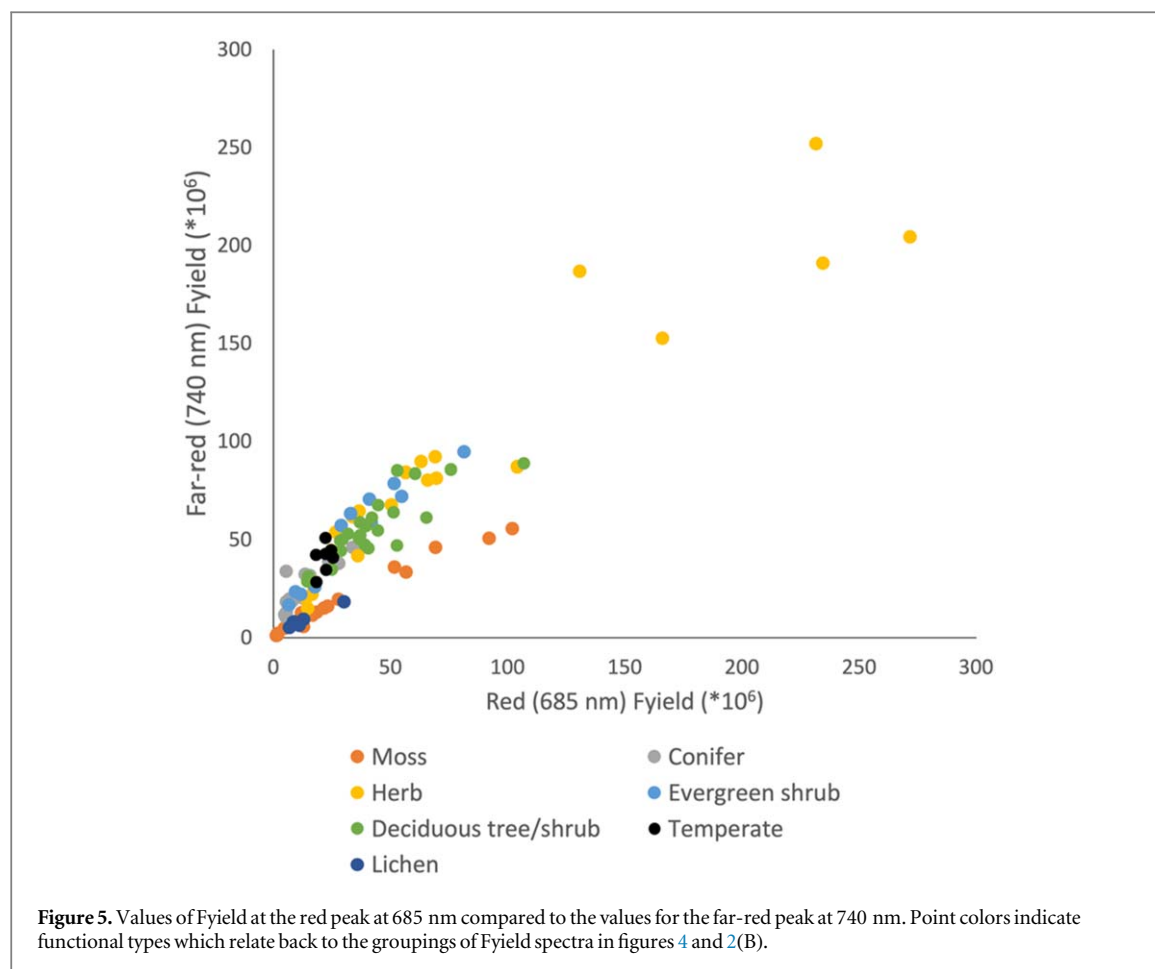shown in figure 2(B), although the temperate samples fall within the range of the Alaskan tree/shrub values. The lichens and mosses have a distinct relationship between the red and far-red Fyield peaks which is different the vascular plants (figure 5). All of the very large herbaceous plant Fyield peak values are from the coltsfoot samples (figure 5). Red and far-red Fyield were strongly correlated, with overall correlation coefficient among the data of r = 0.92. Strongest correlations were for moss and lichen samples (r = 0.99 and 0.97, respectively), while the correlations were lowest for conifers and deciduous shrubs/trees (r = 0.90 and 0.84, respectively).

The ANOVA GLM least square means of the dependent variables are reported in table 2, indicating the significance of the differences among the Fyield means with a different letter. The range of the coefficients of

Figure 5. Values of Fyield at the red peak at 685 nm compared to the values for the far-red peak at 740 nm. Point colors indicate functional types which relate back to the groupings of Fyield spectra in figures 4 and 2(B).

determination (r^2) inform on the level of determination attributed to the ANOVA variables: sample plant functional types, species, sample sources, and their interactions.

Fyield varied significantly among species and with functional type (Mean per PFT, table 2). Coltsfoot (*P. frigidus*) had the highest Fyield, followed by *Eriophorum* spp. from Toolik. Herbaceous plants had the highest Fyields, both for red and far-red peak values, followed by deciduous shrub/tree and mosses, with conifers and lichens together having the lowest Fyield. Fyield varied significantly with functional type, and the combined effect of species*sample source (table 2). Fyield differences in the means among samples from different plant functional types are due to the bio-physical and structural differences among the species. The overall (means of all samples per site) Fyield means at 685 nm and 760 nm measured from samples collected at Fairbanks and Toolik were significantly higher as compared to the Fyield means measured at Utqiaġvik.

In general, species with high Fyield (table 2 bolded entries) had relatively low chlorophyll content.
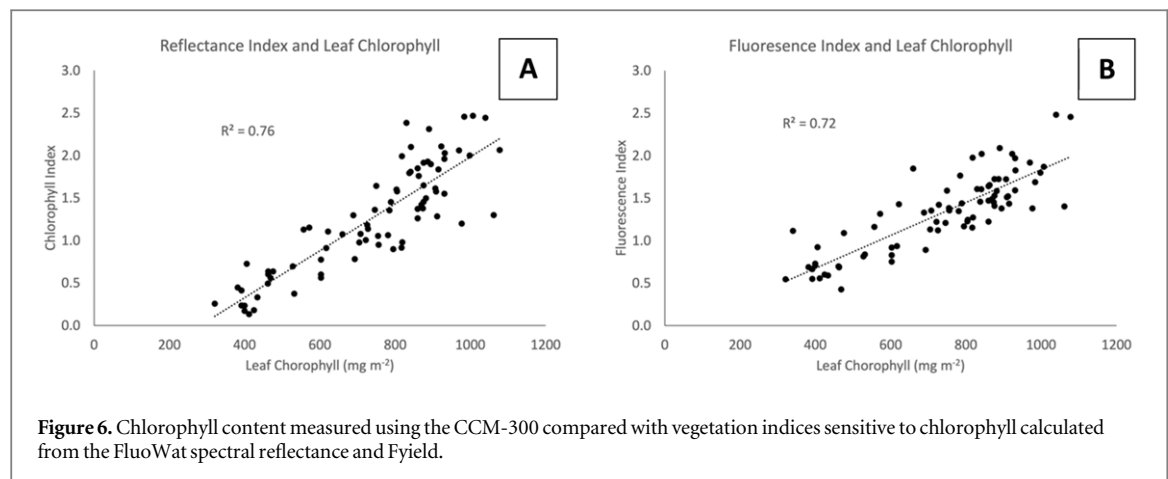
3.3. Detecting chlorophyll content

Chlorophyll content varied significantly among species and functional type (Mean per PFT, table 2). The highest chlorophyll content was measured from *Vaccinium vitis-idea*, followed by *Laris laricina* and *Alnus viridis*. By functional type evergreen shrubs had the highest chlorophyll content, followed by conifers, deciduous shrubs and herbaceous plants, however only the differences between evergreen shrubs and herbaceous plants were statistically significant. In comparison, the chlorophyll content for lichen and moss was significantly lower (e.g., up to 150 mg m^{-2} lower), and there were no significant differences in chlorophyll content between lichen and moss.

Significantly lower mean chlorophyll was measured from the samples from Fairbanks and Toolik, with no significant differences between the means for these sites, as compared to the mean chlorophyll for Utqiagvik.

For the samples measured with the CCM-300 chlorophyll meter, we examined the use of reflectance and fluorescence spectral vegetation indices to detect the leaf chlorophyll content values (figure 6).

The Gitelson Chlorophyll Index (Ci) makes use of reflectance from spectral bands in the red-edge and near infrared wavelength regions (Gitelson *et al* 2006, Ustin *et al* 2009) using the equation

Figure 6. Chlorophyll content measured using the CCM-300 compared with vegetation indices sensitive to chlorophyll calculated from the FluoWat spectral reflectance and Fyield.

$$Ci = \left(\frac{R_{790}}{R_{705}}\right) - 1 \tag{3}$$

where R790 and R705 are the reflectances at 790 and 705 nm respectively. There is a strong relationship of the Ci with chlorophyll content across a wide range of sample types (figure 6(A)).

The Fyields at the individual fluorescence peak red and far-red bands of 685 and 740 nm are poorly correlated with chlorophyll content, with correlation coefficients of -0.34 and -0.10 respectively. The coltsfoot samples have Fyield values far greater than the other samples, but with moderate chlorophyll concentrations, although removing the coltsfoot values only minimally improves the correlations.

Ratios of red and far-red fluorescence bands have been shown to be related to chlorophyll content (Hak *et al* 1990, Lichtenthaler *et al* 1990, D'Ambrosio *et al* 1992, Middleton *et al* 1996). The ratio of peak far-red to red Fyields in this dataset is strongly correlated with measured chlorophyll content (figure 6(B)). This ratio can be visualized in figure 5 as the slope of lines from the origin to each point. The correlation of the far-red to red Fyield with measured chlorophyll content may in part be due to the similarity of this fluorescence ratio to the method used to calculate chlorophyll content in the CCM-300. The CCM-300 uses only a single excitation wavelength, at ~460 nm and measures the ratio of the 735 and 700 nm emissions to determine chlorophyll content, while for the fluorescence chlorophyll index shown in figure 6(B) the samples are illuminated by a wide wavelength range (from ~400 to 650 or 700 nm) and uses the ratio of Fyield at 740 and 685 nm. Future work with a more independent measurement of chlorophyll content is needed to verify these results.

4. Discussion

The spectral reflectance of these high latitude samples frequently varied from the temperate leaf reflectances (figure 2(A) compared to figure 3). In particular, the nonvascular plants, lichens and mosses, displayed reflectance spectra that differed from typical green leaf reflectance with higher and more variable visible reflectances as well as variability due to moisture status. Conifer shoots had lower near infrared reflectances than the deciduous tree leaves (figures 3(C) and (F)). When applying algorithms trained with observations from temperate regions to high latitudes, the significant differences in the reflectance spectra of high latitude plants compared to temperate species represent a potential source of uncertainties when applying algorithms trained with observations from regions outside of the high latitudes. However, the variability in these high latitude sample reflectances also provides a potential source of information for describing vegetation characteristics for this region. Systematic collections of reflectance data are required to make full use of this type of information.

The Fyield spectra also showed significant variability among these high latitude plant types and differences from the temperate leaf Fyield spectra (figure 2(B) compared to figure 4). Many of the samples had Fyield spectral shapes that were quite different than the usual two broad peaks of healthy green leaves. For example, lichens and mosses had no far-red peaks in their Fyield spectra (figures 4(A) and (B)) while the conifer shoots displayed very small red peaks, most likely due to reabsorption of red fluorescence within the needles and shoot (figure 4(C)). Coltsfoot leaves had extremely high Fyield peaks, much larger than any other sample (figure 4(D)). Anecdotally, the coltsfoot leaf measurements correspond to SIF field measurements of ~1 m^2 plots in Utqiagvik that found higher plot-level SIF values in plots dominated by coltsfoot. Further research is required to understand the cause of the high Fyield from coltsfoot.

Table 2. Variation in Fyield at the red peak (685 nm) and far-red peak (740 nm) wavelengths by plant functional type (PFT) and species based on analysis of variances General Linear Models (ANOVA GLM). Statistically significant differences among means within and among PFTs are indicated with different letters (p<0.001, r^2 from 0.78 to 0.92). Source is the location where samples originated, chlorophyll values measured by the CCM-300, n is the number of FluoWat measurements, se is the standard error, sd is the standard deviation, the letters in the columns following the mean values indicate statistically significant differences among means within PFT and among PFTs by the different letters. The species with highest Fyield values per plant functional type are bolded.

PFT *	Species	Source	Fyield 685nm			Fyield 740nm				Chl mg/m^2		
			mean	sd	se	mean	sd	se	n	mean	sd	se
Conifer	Larix laricina	Fairbanks	12.67 a			20.04 a			1	**882.00** b		
	Picea glauca	Fairbanks	28.82 b	9.69	4.84	40.83 b	7.60	3.80	4	781.25 a	60.88	30.44
	Picea mariana	Fairbanks	11.22 a	10.29	3.10	23.65 a	11.92	3.59	3	**860.00** b	21.20	9.76
Deciduous shrub/tree	Alnus rubra	Fairbanks	39.13 a			47.26 a			1	746.00 a		
	Alnus viridis	Fairbanks	34.85 a	7.68	3.84	53.31 b	10.08	5.04	4	**887.00** e	15.56	7.78
	Betula nana	**Toolik**	**52.17** c	1.17	0.83	**74.49** c	15.05	10.64	2	817.50 c	17.68	12.50
	Betula spp.	Fairbanks	39.34 ab	3.82	2.70	55.84 b	7.57	5.36	2	866.50 d	40.31	28.50
	Populus tremuloides	Fairbanks	47.53 b	16.18	5.72	56.68 b	12.78	4.52	8	772.63 b	114.27	40.40
	Salix pulchra	Utqiagvik	43.16 bc	35.66	14.56	54.15 ab	26.95	11.00	6	817.67 c	140.04	57.17
Evergreen shrub	Arctous alpina	Toolik	40.79 b	11.37	6.57	64.71 c	11.93	6.89	3	**930.67** b	123.07	71.05
	Cassiope tetragona	**Toolik**	**68.12** c	18.81	13.30	**83.25** c	15.98	11.30	2	564.50 a	10.61	7.50
	Rhododendron tomentosum	Fairbanks	17.76 a			25.77 a			1	874.00 b		
	Vaccinium vitis-idaea	Fairbanks	22.54 a	17.05	8.52	43.41 b	27.43	13.71	4	998.75 c	75.78	37.89
	Vaccinium vitis-idaea	Toolik	14.41 a	3.74	2.65	24.55 a	3.66	2.58	2	969.00 c	53.74	38.00
Herbaceous plants	Arctophila fulva	Utqiagvik	66.36 b	4.64	3.28	85.42 c	5.88	4.16	2	761.50 c	47.38	33.50
	Carex aquatilis	Toolik	48.53 ab	18.29	10.56	66.20 bc	14.87	8.59	3	793.00 cd	77.70	44.86
	Carex aquatilis	Utqiagvik	46.34 ab	14.44	10.21	62.89 b	30.05	21.25	2	843.50 d	37.48	26.50
	Eriophorum spp.	Fairbanks	15.08 a	1.36	0.78	18.94 a	3.75	2.16				
	Eriophorum spp.	**Toolik**	**104.16** c			**87.07** c			1	532.00 a		
	Eriophorum spp.	Utqiagvik	25.67 a	1.41	1.00	49.09 b	6.72	4.75	2	**960.50** e	53.03	37.50
	Petasites frigidus	**Toolik**	**184.04** d	75.99	31.02	**179.66** d	53.71	21.93	6	586.83 b	74.76	30.52
	Petasites frigidus	Utqiagvik	29.32 a	10.27	5.93	51.45 b	20.20	11.66	3	852.67 d	74.19	42.83
Lichen	Cladonia rangiferina	Fairbanks	12.61	7.99	3.02	8.73	4.35	1.64	4	409.25	11.93	5.96
Moss	**Hylocomnium splendens**	**Toolik**	**87.80** b	16.77	9.68	50.71 b	4.79	2.77	3	368.33 a	40.99	23.67
	Sphagnum spp.	Fairbanks	20.51 a	18.06	5.45	13.97 a	11.28	3.40	6	**449.50** b	24.63	10.06
	Sphagnum spp.	Toolik	10.48 a	15.03	8.68	7.56 a	10.29	5.94	2	361.50 a	28.99	20.50
Mean^2 per PFT	*Conifer*		17.57 a	9.99	3.97	28.18 b	9.76	3.70	7	841.08 cb	30.44	15.22
	Deciduous shrub/tree		42.70 c	12.90	5.53	56.95 c	14.49	7.31	23	817.88 bc	65.57	29.27
	Evergreen shrub		32.72 b	12.74	7.76	48.34 c	14.75	8.62	12	867.38 c	65.80	38.61
	Herbaceous plants		**64.94** d	18.06	8.97	**75.09** d	19.31	10.64	19	761.43 b	60.76	35.95
	Lichen		12.61 a	7.99	3.02	8.73 a	4.35	1.64	4	409.25 a	11.93	5.96
	Moss		39.60 bc	16.62	7.93	24.08 b	8.79	4.04	11	393.11 a	31.54	18.07

The variability in Fyield spectra points to the potential to use these data to separate different high latitude plant functional types. The AVOVA analysis of the Fyield peak values showed significant differences among the functional types in this data collection (table 2). Again, further data collections are required to advance this technique.

Individual Fyield peak bands poorly correlated with leaf chlorophyll content (r = −0.34 and −0.10 for red and far-red peak bands respectively). Some imagers used for remote sensing of SIF, such as the Chlorophyll Fluorescence Imaging Spectrometer (CFIS) and Orbiting Carbon Observatory 2 (OCO2) only provide measurements of far-red SIF and these results suggest they may not be able to provide good descriptions of chlorophyll content in high latitude landscapes. However, despite the high variability in reflectance and Fyield spectra of these samples, both reflectance and fluorescence indices were found to be strongly related to chlorophyll content (figure 6). The ability of these indices to determine chlorophyll content from remote sensing spectral imagery offers the potential for describing patterns of tundra productivity across the landscape. Huemmrich *et al* (2013) found that the Gitelson Chlorophyll Index (Ci, equation (3)) was strongly correlated with tundra photosynthetic light use efficiency calculated from estimations of cover fractions based on 30 m satellite spectral imagery.

For these high latitude plant samples both reflectance and fluorescence data have been shown to be able to describe chlorophyll content and plant functional types. This points to the potential of combining these two different types of optical information to improve retrievals of landscape characteristics, fill in data gaps, and for temporal and spatial scaling.

5. Conclusions

High latitude vegetation displays wide variations in spectral reflectance and Fyield spectral shapes at the leaf level. This variability may provide information for remote sensing of vegetation type but may also confound

attempts to measure high latitude vegetation characteristics and function. Further, leaf level reflectance and Fyield values from high latitude plants can significantly differ from those of typical temperate plants, potentially resulting in errors in retrieval algorithms trained with data from other regions when applied to high latitude ecosystems.

Despite the variability in the reflectance and Fyield spectral shapes among these samples, indices using these data were able to describe the variability in leaf chlorophyll content. The ability to determine chlorophyll content from remote sensing spectral imagery may be useful in describing patterns of tundra productivity.

This study provides a first step examining Fyield for common high latitude species and examples of different plant functional types, providing an initial step for up-scaling of SIF and chlorophyll content from leaf-level to canopy and airborne/space-borne levels. Recent flight campaigns of NASA's Arctic-Boreal Vulnerability Experiment (ABoVE) have produced an unprecedented collection of spectral reflectance imagery from the Airborne Visible/Infrared Imaging Spectrometer Next Generation (AVIRIS NG) along with images of solar induced fluorescence (SIF) from the Chlorophyll Fluorescence Imaging Spectrometer (CFIS) of high latitude boreal forest and tundra landscapes in Alaska and northwestern Canada (Miller *et al* 2019) to advance these studies. Further research is needed, using these data in synergy with land cover plant functional type and species maps, to associate Fyield characteristics established in this study with their spatial location and coverage.

Acknowledgments

ORCID iDs

K Fred Huemmrich ⓘ https://orcid.org/0000-0003-4148-9108
Sergio A Vargas Z ⓘ https://orcid.org/0000-0002-0052-8580
Steven Unger ⓘ https://orcid.org/0000-0002-9562-8209

References

Beamish A *et al* 2020 Recent trends and remaining challenges for optical remote sensing of Arctic tundra vegetation: a review and outlook *Remote Sens. Environ.* **246** 111872
Bornman J F, Vogelmann T C and Martin G 1991 Measurement of chlorophyll fluorescence within leaves using a fibreoptic microprobe *Plant Cell Environ.* **14** 719–25
Bratsch S N, Epstein H, Buchhorn M and Walker D 2016 Differentiating among four arctic tundra plant communities at Ivotuk, Alaska using field spectroscopy *Remote Sens.* **8** 51
Bratsch S N, Epstein H, Buchhorn M, Walker D and Landes H 2017 Relationships between hyperspectral data and components of vegetation biomass in Low Arctic tundra communities at Ivotuk, Alaska *Environ. Res. Lett.* **12** 025003
Brown J, Everett K R, Webber P J, MacLean S F Jr and Murry D F 1980 The coastal tundra at barrow in an arctic ecosystem, the coastal tundra at barrow, Alaska 1–29 ed J Brown *et al* (Stroudsberg, PA: Dowden, Hutchison, and Ross, Inc)
Buchhorn M, Walker D, Heim B, Raynolds M K, Epstein H and Schwieder M 2013 Ground-based hyperspectral characterization of Alaska tundra vegetation along environmental gradients *Remote Sens.* **5** 3971–4005
D'Ambrosio N, Szabo K and Lichtenthaler H K 1992 Increase in the chlorophyll fluorescence ratio F690/F735 during the autumnal chlorophyll breakdown *Radiot. Environ. Biophys.* **31** 51–62
Frankenberg C *et al* 2011 New global observations of the terrestrial carbon cycle from GOSAT: patterns of plant fluorescence with gross primary productivity *Geophys. Res. Lett.* **38** L17706
Gitelson A A, Buschmann C and Lichtenthaler H K 1999 The chlorophyll fluorescence ratio F735/F700 as an accurate measure of the chlorophyll content in plants *Remote Sens. Environ.* **69** 296–302
Gitelson A A, Keydan G P and Merzlyak M N 2006 Three-band model for non-invasive estimation of chlorophyll, carotenoids, and anthocyanin contents in higher plant leaves *Geophys. Res. Lett.* **33** L11402
Green T G A and Lange O L 1995 Photosynthesis in poikilohydric plants: a comparison of lichens and bryophytes In *Ecophysiology of Photosynthesis* (Berlin Hedelberg: Springer) 100, 319–41
Hak R, Lichtenthaler H K and Rinderle U 1990 Decrease of the fluorescence ratio F690/F730 during greening and development of leaves *Radiot. Environ. Biophys.* **29** 329–36
Hollister R D, Webber P J and Tweedie C E 2005 The response of Alaskan arctic tundra to experimental warming: Differences between short- and long-term responses *Global Change Bio.* **11** 525–36
Hope A S and Stow D A 1996 Shortwave reflectance properties of arctic tundra landscapes In *Landscape Function and Disturbance in Arctic Tundra.* (Berlin Hedelberg: Springer) 120, 155(164:
Huemmrich K F, Gamon J A, Tweedie C E, Campbell P K E, Landis D R and Middleton E M 2013 Arctic tundra vegetation functional types based on photosynthetic physiology and optical properties *IEEE J. Select, Topics Applied Earth Obs. and Remote Sens.* **6** 265–75

Jeong S J, Schimel D, Frankenberg C, Drewry D T, Fisher J B, Verma M, Berry J A, Lee J E and Joiner J 2017 Application of satellite solar-induced chlorophyll fluorescence to understanding large-scale variations in vegetation phenology and function over northern high latitude forests *Remote Sens of Environ.* **190** 178–87

Joiner J *et al* 2014 The seasonal cycle of satellite chlorophyll fluorescence observations and its relationship to vegetation phenology and ecosystem atmosphere carbon exchange *Remote Sens. Environ.* **152** 375–91

Lichtenthaler H K, Hak R and Rinderle U 1990 The chlorophyll fluorescence ratio F690/F730 in leaves of different chlorophyll content *Photosyn. Res.* **25** 295–8

Middleton E M, Chan S S, Rusin R J and Mitchell S K 1997 Optical properties of black spruce and Jack pine needles from conifer stands at the BOREAS tower sites in Saskatchewan *Canada Canadian J. Remote Sensing.* **23** 108–19

Middleton E M, Chappelle E W, Cannon T A, Adamse P and Britz S J 1996 Initial assessment of physiological response to UV-B irradiation using fluorescence measurements *J. Plant Physiol.* **148** 68–77

Middleton E M, Huemmrich K F, Zhang Q, Campbell P K E and Landis D R 2018 Spectral bio-indicators of photosynthetic efficiency and vegetation stress chap. 5 ed P S Thenkabail, J G Lyon and A Huete *Hyperspectral Remote Sensing of Vegetation Biophysical and Biochemical Characterization and Plant Species Studies* (New York, NY: Taylor & Francis) 2nd edition III, 133–79

Middleton E M, Walter-Shea E A, Mesarch M A, Chan S S and Rusin R J 1998 Optical properties of canopy elements in black spruce, jack pine, and aspen stands at BOREAS sites in Saskatchewan, Canada *Canadian J. Rem. Sens.* **24** 169–86

Miller C E *et al* 2019 An overview of ABoVE airborne campaign data acquisitions and science opportunities *Environ. Res. Lett.* **14** 080201

Mohammed G H *et al* 2019 Remote sensing of solar-induced chlorophyll fluorescence (SIF) in vegetation: 50 years of progress *Remote Sen. Env.* **231** 111177

Murata N, Nishimura M and Tamiya A 1966 Fluorescence of chlorophyll in photosynthetic systems. III. Emission and action spectra of fluorescence - three emission bands of chlorophyll a and the energy transfer between two pigment systems *Biochim. Biophys. Acta* **126** 234–43

Myers-Smith I *et al* 2011 Shrub expansion in tundra ecosystems: dynamics, impacts and research priorities *Environ. Res. Lett.* **6** 45509

Myers-Smith I *et al* 2020 Complexity revealed in the greening of the Arctic *Nat. Clim. Chang.* **10** 106–17

Pfündel E 1998 Estimating the contribution of photosystem I to total leaf chlorophyll fluorescence *Photosynth. Res.* **56** 185–95

Prevéy J *et al* 2017 Greater temperature sensitivity of plant phenology at colder sites: implications for convergence across northern latitudes *Glob. Change Bio.* **23** 2660–71

Rautiainen M, Lukeš P, Homolová L, Hovi A, Pisek J and Mõttus M 2018 Spectral properties of coniferous forests: a review of *in situ* and laboratory measurements *Remote Sens.* **10** 207

Smith R L 2008 *Interior and Northern Alaska* (Bothell WA: A Natural History Book Publishers Network)

Stow D A, Burns B H and Hope A S 1993 Spectral, spatial and temporal characteristics of Arctic tundra reflectance *Int. J. of Remote Sens.* **14** 2445–62

Tenhunen J D, Siegwolf R T W and Oberbauer S F 1995 Effects of phenology, physiology, and gradients in community composition, structure, and microclimate on tundra ecosystem CO2 exchange *Ecophysiology of Photosynthesis* ed E-D Schulze and M M Caldwell (Berlin Heidelberg: Springer) p.431–460

Ustin S L, Gitelson A A, Jacquemoud S, Schaepman M, Asner G P, Gamon J A and Zarco-Tejada P 2009 Retrieval of foliar information about plant pigment systems from high resolution spectroscopy *Remote Sens. Environ.* **113** S67–77

Walker M D, Walker D A and Auerbach N A 1994 Plant communities of a tussock tundra landscape in the brooks range foothills *Alaska Journal of Veg. Sci.* **5** 843–66

Williams D L 1991 A comparison of spectral reflectance properties at the needle, branch, and canopy level for selected conifer species *Remote Sens. Environ.* **35** 79–93

Van Wittenberghe S, Alonso L, Verrelst J, Hermans I, Delegido J, Veroustraete F, Valcke R, Moreno J and Samson R 2013 Upward and downward solar-induced chlorophyll fluorescence yield indices of four tree species as indicators of traffic pollution in Valencia *Environ. Pollut.* **173** 29–37

Van Wittenberghe S, Alonso L, Verrelst J, Moreno J and Samson R 2015 Bidirectional sun-induced chlorophyll fluorescence emission is influenced by leaf structure and light scattering properties - a bottom-up approach *Remote Sens. Environ.* **158** 169–79

Zar J H 2010 *Biostatistical Analysis* 5th Edition (Saddle River: Prentice-Hall/Pearson Upper) p.944